"N-Fused Porphyrin": A New Tetrapyrrolic Porphyrinoid with a Fused Tri-pentacyclic Ring

Hiroyuki Furuta,*,†,‖ Tomoya Ishizuka,† Atsuhiro Osuka,*,† and Takuji Ogawa‡,§

Contribution from Department of Chemistry, Graduate School of Science, Kyoto University, Kyoto 606-8502, Japan, PRESTO, JST, and Institute for Fundamental Research of Organic Chemistry (IFOC), Kyushu University, Fukuoka 812-8581, Japan

Received January 13, 2000

Abstract: The syntheses and X-ray structures of novel porphyrinoids, "N-fused porphyrins (NFPs)", and their reactivity were described. NFP was spontaneously produced from the bromo-substituted N-confused tetraarylporphyrin in a pyridine solution at room temperature. X-ray diffraction analyses revealed that the porphyrinoid core containing a fused tri-pentacyclic ring is almost planar. The deviation from the mean plane of **4e′**, for example, was within 0.30 Å. The peripheral aryl substituents were tilted 50.4, 53.5, 64.4, and 12.4° relative to the porphyrin mean plane, respectively. The occurrence of a three-centered hydrogen bonding in the NFP core was inferred by the downfield shift of the inner NH signal (e.g., 8.48 ppm for **4e′**) in ^{1}H NMR and the short distances (within 2.4−2.9 Å) among the inner core nitrogens, N_2, N_3, and N_4. The optical absorption spectra of NFPs exhibit Soret-like transitions around 360, 500, and 550 nm and weak Q-like bands around 650, 700, 850, and 940 nm in CH_2Cl_2. The electrode process of **4e′** showed the first oxidation at 0.08 V and reduction at −1.37 V (vs Fc/Fc^+), which suggested the small energy gap attributed to the unusual long-wavelength absorption was mainly due to the rising of the HOMO energy level. The first-order rate constants (k_f) for the transformation from NCPs to NFPs were largely affected by the substituents at the meso position, showing a good correlation with Hammet σ^+ parameters. Moreover, the reverse reaction from NFPs to NCPs was observed in the CH_2Cl_2 solution by treating with a base. Dynamic ring inversion in the tetrapyrrolic porphyrin core is discussed.

Introduction

Porphyrin, a representative of tetrapyrrolic macrocycle, is well-characterized by the square planar arrangement of a set of pyrrolic nitrogens in the core. The recent studies of a variety of porphyrin analogues, however, have been gradually revealing the structural versatility of porphyrinoids.[1] For example, octaphyrin, a member of so-called expanded porphyrins, exhibits a twisted conformation of figure eight type.[2] Even with a smaller hexapyrrolic porphyrinoid, hexaphyrin, the "inverted" conformation, where a pair of pyrrolic NH's pointed outward from the core, was reported.[3,4] Moreover, with sapphyrin, a pentapyrrolic corrole, was shown the dynamic inversion of pyrrolic rings in a core.[5] Such findings gave us the impression that porphyrinoids with larger core possess higher structural flexibility (Chart 1).[6]

During the study of the inverted porphyrin isomer, "N-confused porphyrin (NCP)", we have been aware of distortion from the planarity due to the repulsion in the core.[7−9] For example, the "confused" pyrrole ring of N-confused

† Kyoto University.

‖ PRESTO, JST.

‡ Kyushu University.

§ Present address: The Department of Chemistry, Ehime University, Ehime 790-8577, Japan.

(1) For overviews of porphyrin analogues, see: (a) Johnson, A. W. In *Porphyrins and Metalloporphyrins*; Smith, K. M., Ed.; Elsevier: Amsterdam, 1975; Chapter 18. (b) Grigg, R. In *The Porphyrins*; Dolphin, D., Ed.; Academic Press: New York, 1978; Chapter 10. (c) Sessler, J. L.; Weghorn, S. J. *Expanded, Contracted & Isomeric Porphyrins*; Tetrahedron Organic Chemistry Series, Vol. 15; Pergamon: New York, 1997. (d) *The Porphyrin Handbook*; Kadish, K. M., Smith, K. M., Guilard, R., Eds.; Academic Press: San Diego, 1999; Vol. 2.

(2) (a) Vogel, E.; Bröring, M.; Fink, J.; Rosen. D.; Schmickler, H.; Lex, J.; Chan K. W. K.; Wu, Y.-D.; Plattner, D. A.; Nendel, M.; Houk, K. N. *Angew. Chem., Int. Ed. Engl.* **1995**, *34*, 2511−2514. (b) Bröring, M.; Jendrny, J.; Zander, L.; Schmickler, H.; Lex, J.; Wu, Y.-D.; Plattner, D. A.; Houk, K. N.; Vogel, E. *Angew. Chem., Int. Ed. Engl.* **1995**, *34*, 2515−2517.

(3) Neves, M. G. P. M. S.; Martins, R. M.; Tome, A. C.; Silvestre, A. J. D.; Silva, A. M. S.; Felix, V.; Drew, M. G. B.; Cavaleiro, J. A. S. *Chem. Commun.* **1999**, 385−386.

(4) At present, three types of "pyrrole inversion" are seen in the literatures: (i) position exchange of acetic and propionic acid groups in the biosynthetic pathway of uroporphyrinogen III from porphobilinogen (Franck, B. *Angew. Chem., Int. Ed. Engl*. **1982**, *21*, 343−353), (ii) change of linkage from α−α to α−β in the polypyrrole macrocycle (Schmacher, K.-H.; Frank, B. *Angew. Chem., Int. Ed. Engl*. **1989**, *28*, 1243−1245), and (iii) rotation of the pyrrolic ring from an inward pointing nitrogen to the outward pointing arrangement.[3]

(5) (a) Chmielewski, P. J.; Latos-Grażyński, L.; Rachlewicz, K. *Chem. Eur. J.* **1995**, *1*, 68−72. (b) Rachlewicz, K.; Spurtta, N.; Latos-Grażyński, L.; Chmielewski, P. J.; Szterenberg, L. *J. Chem. Soc., Perkin Trans. 2* **1998**, 959−967.

(6) For convenience, the same compound numbers with "prime" symbol were used for tolyl derivatives, e.g., **3a** (Ar = phenyl) and **3a′** (Ar = tolyl).

(7) (a) Furuta, H.; Asano, T.; Ogawa, T. *J. Am. Chem. Soc.* **1994**, *116*, 767−768. (b) Ariga, K.; Kunitake, T.; Furuta, H. *J. Chem. Soc., Perkin Trans. 2*, **1996**, 667−672. (c) Ishikawa, Y.; Yoshida, I.; Akaiwa, K.; Koguchi, E.; Sasaki, T.; Furuta, H. *Chem. Lett.* **1997**, 453−454. (d) Furuta, H.; Ogawa, T.; Uwatoko, Y.; Araki, K. *Inorg. Chem.* **1999**, *38*, 2676−2682. (e) Doubly N-confused porphyrins have been synthesized recently: Furuta, H.; Maeda, H.; Osuka, A. *J. Am. Chem. Soc.* **2000**, *122*, 803−807.

(8) (a) Chmielewski, P. J.; Latos-Grażyński, L.; Rachlewicz, K.; Glowiak, T. *Angew. Chem., Int. Ed. Engl*. **1994**, *33*, 779−781. (b) Chmielewski, P. J.; Latos-Grażyński, L. *J. Chem. Soc., Perkin Trans. 2* **1995**, 503−509. (c) Chmielewski, P. J.; Latos-Grażyński, L.: Glowiak, T. *J. Am. Chem. Soc.* **1996**, *118*, 5690−5701. (d) Chmielewski, P. J.; Latos-Grażyński, L. *Inorg. Chem.* **1997**, *36*, 840−845. (e) Latos-Grażyński, L. In *The Porphyrin Handbook*; Kadish, K. M., Smith, K. M., Guilard, R., Eds; Academic Press: San Diego, 1999; Vol. 2, Chapter 14.

10.1021/ja000148i CCC: $19.00
Published on Web 05/31/2000

Chart 1

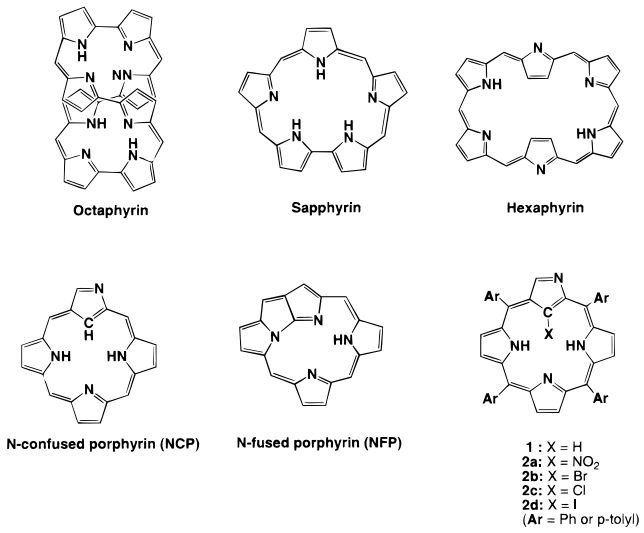

tetraphenylporphyrin (NCTPP, **1**) is tilted 26.9° from the porphyrin plane and that of nitro-substituted NCP, **2a**, is canted 42.4° (Figure 1).[7a,10] While investigating the correlation between the size of a substituent at the inner carbon and the degree of NCP deformation using a series of inner halide derivatives, we have observed the spontaneous formation of a new type of porphyrinoid, N-fused porphyrin (NFP), from the brominated NCP.[11] NFP possesses a characteristic fused tri-pentacyclic ring in the macrocyclic core and exhibits the unusual long-wavelength absorption near 1000 nm. Mechanistically, the fused ring was supposed to be formed by the inversion of the confused pyrrole ring in the NCP core. In this paper, we report the details of syntheses, structures, kinetics of NFP formation, and the inversion property of NCP and NFP. To the best our knowledge, this is the first example of the dynamic inversion of a pyrrolic group in a tetrapyrrolic framework.

Results and Discussion

Halogenation of NCP. The previous finding of the facile nitration at the inner carbon of NCTPP (**1**) prompted us to further investigate electrophilic substitution on that carbon.[7c] A series of halogenation reactions with *N*-halosuccinimide derivatives have been attempted. When a CH_2Cl_2 solution of **1** was treated with 1 equiv of NBS for 5 min at room temperature, the monobrominated NCTPP, **2b**, was obtained in over 90% yield. Further, the addition of 2 equiv of NBS afforded the dibrominated NCTPP, **3b**, in 70% yield (Scheme 1).

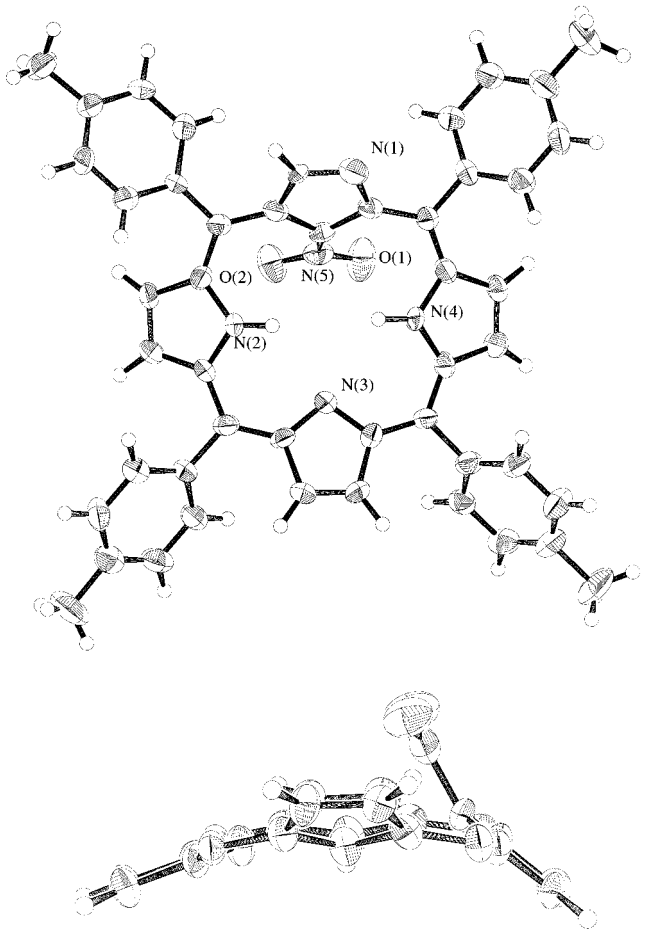

Figure 1. X-ray structures of **2a′**: top view (upper) and side view (below). Aryl groups were omitted for clarity in the side view.

Scheme 1

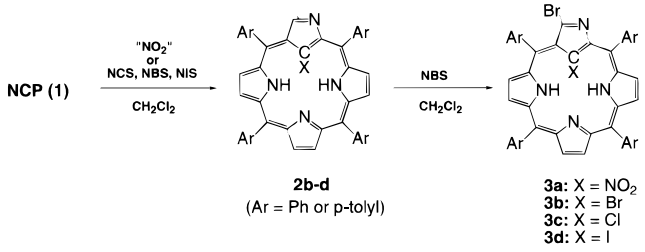

The bromination proceeded regioselectively, i.e., first, at the inner carbon and, then, at the outer α-position of the confused pyrrole ring. For both **2b** and **3b**, the ^{1}H NMR signal of the inner CH, which was observed at −5.1 ppm in **1**, was not found. In addition, a singlet signal at 7.23 ppm, ascribed to the outer α-H of the confused pyrrole ring in **2b**, also disappeared in the dibrominated species **3b**. When *N*-chlorosuccinimide (NCS) and *N*-iodosuccinimide (NIS) were used in place of NBS, the corresponding mono halo-NCTPPs, **2c** and **2d**, were formed but the dihalogenated products such as **3b** were not obtained under the same conditions, presumably due to the low reactivity of NCS and the instability of the diiodo derivative.

Inner C-halogenated NCTPPs, **2b** and **2c**, gave absorption spectra similar to the starting free base, but the bands were broadened and bathochromically shifted. For example, the absorption maxima of Soret bands of **1** and **2b**,**c** were observed at 438.0, 453.0, and 449.5 nm, respectively.[12] Such changes could reflect the distortion of the porphyrin ring from the plane due to the tilt of the confused pyrrole ring. Furthermore, both

(9) (a) Hoo, P.-Y.; Shin, K.; Lee, C.-H. *Tetrahedron Lett.* **1996**, *37*, 197−200. (b) Lee, C.-H.; Kim, H.-J. *Tetrahedron Lett.* **1997**, *38*, 3935−3938. (c) Liu, B. Y.; Brückner, C.; Dolphin, D. *J. Chem. Soc., Chem. Commun.* **1996**, 2141−2142. (d) Narayanan, S. J.; Sridevi, B.; Srinivasan, A.; Chandrashekar, T. K.; Roy, R. *Tetrahedron Lett.* **1998**, *39*, 7389−7392. (e) Geier, G. R., III; Lindsey, J. L. *J. Org. Chem.* **1999**, *64*, 1596−1603. (f) Geier, G. R., III; Haynes, D. M.; Lindsey, J. S. *Org. Lett.* **1999**, *1*, 1455−1458. (g) Lash, T. D.; Richter, T. D.; Shiner, C. M. *J. Org. Chem.* **1999**, *64*, 7973−7982.

(10) First reported by: Furuta, H.; Tsuruoka, S. 28th Congress of Heterocyclic Chemistry, Shizuoka, October 1997, 366−369. The datum crystal was a green prism obtained from a CH_2Cl_2/CH_3OH solution of **2a**. Crystal data for **2a**: $C_{49}H_{41}N_5O_3$, Mw = 747.89, triclinic, space group, *P*1, with a = 14.325(7) Å, b = 14.773(6) Å, c = 9.720(4) Å, α = 104.95(3)°, β = 103°, γ = 93°, V = 1920(1) Å^3, Z = 2, μ = 0.817 cm^{-1}, D_{calc} = 1.294 g/cm^3, and crystal dimensions 0.20 × 0.20 × 0.20 mm. The data were collected on Rigaku Afc.5r diffractometer at 25.0 °C, and the structure was solved by direct methods. It refined to R = 0.062, R_w = 0.046, GOF = 1.810 for 7168 with $I > 3.0\ \sigma(I)$.

(11) Furuta, H.; Ishizuka, T.; Osuka, A.; Ogawa, T. *J. Am. Chem. Soc.* **1999**, *121*, 2945−2946.

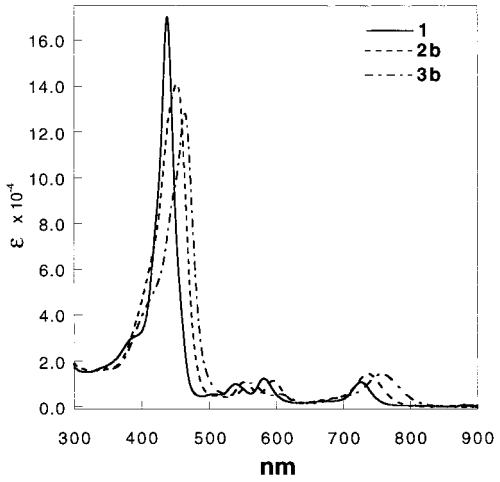

Figure 2. Absorption spectra of **1**, **2b**, and **3b** in CH_2Cl_2.

Scheme 2

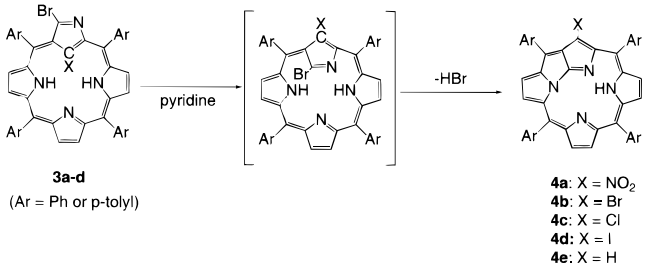

Soret and Q transitions were bathochromically shifted to 465 and 757 nm (Figure 2), respectively, in the dibrominated species **3b**.

N-Fused Porphyrin (NFP) from N-Confused Porphyrin (NCP). Dibrominated NCP, **3b**, was found to be unstable in solution, such that the starting green solution gradually changed to red. The reaction proceeded spontaneously and was completed in 8 h at room temperature in pyridine. The structure of the product was explicitly revealed by X-ray single-crystal analysis (vide infra), which showed a fused tri-pentacyclic ring and two pyrrolic rings in a macrocyclic core. Based on this unique skeleton, we named this compound "N-fused porphyrin, NFP". From the mechanistic point of view, the reaction seemed to proceed by the inversion of the confused pyrrole ring, followed by the nucleophilic attack of the adjacent pyrrole and subsequent elimination of HBr (Scheme 2).[13]

The second bromination at the outer α-carbon seems to be critical for the ring fusing process that leads to NFP formation. In fact, by treatment with 1 equiv of NBS, C-nitro-substituted NCP **2a** and C-chloro derivative **2c** were changed to the NFP derivatives **4a** and **4c**, respectively. In both cases, the brominated intermediates **3a** and **3c** were isolated and the transformation to **4a** occurred within 3 h at 80 °C and to **4c** within 8 h at room temperature in pyridine solution, respectively. When NCS and NIS were used in place of NBS at the second halogenation step in Scheme 1, the chlorination or iodination at the outer α-carbon of **2a**−**d** did not proceed in CH_2Cl_2 solution at room temperature, precluding the preparation of NFPs from this route.

When 2 equiv of NBS was added to the solution of **4b**, tribrominated NFP **5b** was obtained quantitatively (Scheme 3).

(12) Iodo derivative **2d** was too unstable to measure the absorption spectrum correctly, but the corresponding anisyl-substituted NCPs were stable, and they gave a similar tendency; 443.0 (FB), 453.8 (Cl), 457.8 (Br), and 465.0 nm (I). Furuta, H.; Tsuruoka, S. Unpublished data.

(13) Due to the resemblance of UV/vis spectra and the weak parent mass peak of **3b**, the NFP formation reaction was considered to proceed from **2b** and succeeding removal of H_2 in the preliminary communication.[11]

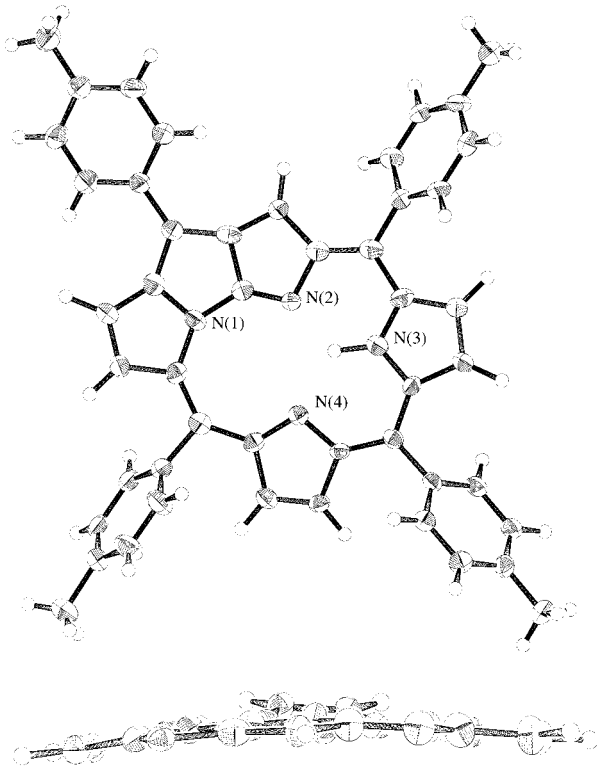

Figure 3. X-ray structures of **4e′**: top view (upper) and side view (below). Aryl groups were omitted for clarity in the side view.

Scheme 3

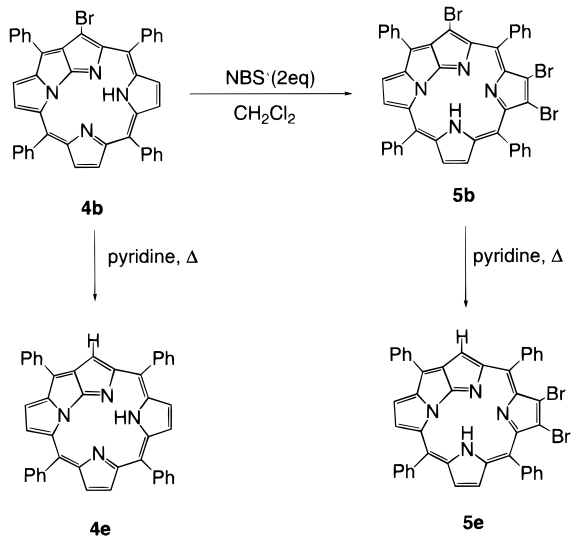

Interestingly, the Br substituent at the tri-pentacyclic ring of **4b** and **5b** could be replaced by hydrogen simply by refluxing in pyridine, affording **4e** and **5e**, respectively. The origin of hydrogen might be derived from the adventitious water in the solvent because when the deuterated water was added to the pyridine solution, the deuterium was introduced in the same position of the NFP ring.

X-ray Structures of NFPs. The structures of NFP derivatives, **4a′**, **4b**, **4e′**, **5b**, and **5e** were revealed by X-ray diffraction analyses. For a representation, ORTEP structures of the unsubstituted NFP, **4e′**, are shown in Figure 3. The porphyrinoid core is almost planar, and the deviation from the mean plane consisting of 24 atoms is within 0.30 Å. The bond length between N_2 and C_9, 1.260 Å, is shorter than other pyrrolic

Chart 2

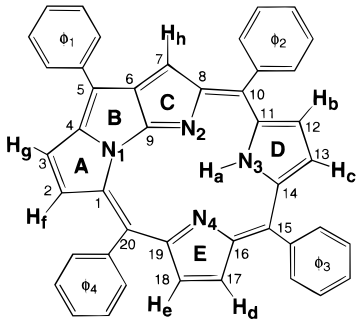

Table 1. Selected Bond Lengths (Å) and Angles (deg) for **4a′**, **4b**, **4e′**, **5b**, and **5e**

	4a′	**4b**	**4e′**	**5b**	**5e**
			Distances, Å		
N_2-C_9	1.31(1)	1.265(7)	1.260(7)	1.29(3)	1.284(9)
N_3-C_{11}	1.36(1)	1.346(7)	1.358(6)	1.41(2)	1.342(7)
N_3-C_{14}	1.40(1)	1.375(7)	1.343(6)	1.41(3)	1.346(9)
N_4-C_{16}	1.36(1)	1.379(7)	1.386(6)	1.43(3)	1.390(9)
N_4-C_{19}	1.33(1)	1.355(7)	1.338(6)	1.35(3)	1.399(8)
$C_{11}-C_{12}$	1.45(1)	1.429(8)	1.420(8)	1.42(3)	1.435(9)
$C_{12}-C_{13}$	1.38(1)	1.351(9)	1.399(7)	1.37(3)	1.44(1)
$C_{13}-C_{14}$	1.43(1)	1.420(8)	1.440(7)	1.41(3)	1.448(8)
$C_{16}-C_{17}$	1.53(1)	1.492(8)	1.454(6)	1.43(2)	1.406(9)
$C_{17}-C_{18}$	1.30(1)	1.247(8)	1.336(7)	1.41(4)	1.367(9)
$C_{18}-C_{19}$	1.54(1)	1.500(8)	1.473(6)	1.44(3)	1.395(9)
$N_2\cdots N_3$	2.47	2.475	2.469	2.54	2.558
$N_3\cdots N_4$	2.63	2.634	2.665	2.74	2.719
$N_2\cdots N_4$	2.98	2.884	2.901	2.78	2.799
			Angles, deg		
$C_{11}N_3C_{14}$	113.7(8)	110.5(4)	111.7(4)	103(2)	109.2(5)
$C_{16}N_4C_{19}$	109.6(7)	105.1(4)	106.8(4)	112(7)	110.1(5)

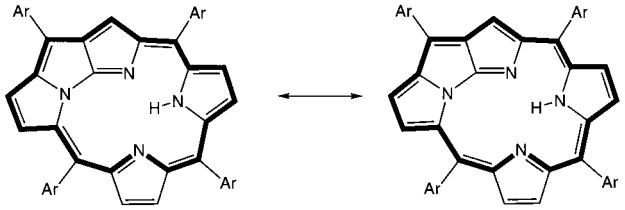

Figure 4. 18 π aromatic circuit of NFP

C−N's (1.34−1.38 Å), which suggests the localization of the double bond in this region (Chart 2, Table 1). Thus, an 18π electron aromatic circuit using peripheral conjugation is plausible (Figure 4).

The tolyl substituents at the meso position (Φ_2, Φ_3, and Φ_4) are tilting 50.4, 53.5, and 64.4° to the porphyrin mean plane, respectively. Those values are similar to that of TPP, ca. 60° (Table 2).[14] On the other hand, the tolyl group on the tri-pentacyclic ring Φ_1 is 12.4° inclined and almost coplanar to the porphyrin plane. The difference might be explained by the steric interaction between *o*-H's of the tolyl group and adjacent pyrrolic β-H's. That is, a narrower inner angle can decrease the rotation barrier of the tolyl group increasing the π overlap with the porphyrin ring. This effect can be observed at the Φ_1 position where the $\angle C_4-C_5-C_6$, is only 103.7°, while at the meso positions $\angle C_8-C_{10}-C_{11}$, $\angle C_{14}-C_{15}-C_{16}$, and $\angle C_{19}-C_{20}-C_1$, are 120.9, 122.2, and 133.9°, respectively. Consequently, the bond length between Φ_1 and C_5 (1.438 Å) is slightly shorter than the bonds between the meso-carbon atoms and the Φ_2, Φ_3 and Φ_4 groups (1.475−1.496 Å).

(14) Silvers, S. J.; Tulinsky, A. *J. Am. Chem. Soc*. **1967**, *89*, 3331−3337.

Table 2. Dihedral Angles between *meso*-Phenyl Groups and the Least-Squares Plane of the Porphyrin Core (deg) (Top) and Bond Lengths (Å) between Phenyl Groups and *meso*-Carbons (Bottom)

	Φ_1	Φ_2	Φ_3	Φ_4
4a′	31.02	75.00	39.43	73.80
	1.49(1)	1.52(1)	1.48(1)	1.51(1)
4b	31.428	64.18	124.32	74.73
	1.463(8)	1.461(7)	1.494(7)	1.520(8)
4e′	12.38	129.64	53.48	115.66
	1.438(7)	1.476(7)	1.475(7)	1.496(7)
5b	29.84	118.10	62.31	77.43
	1.49(3)	1.51(2)	1.50(3)	1.50(3)
5e	17.40	128.08	124.28	71.68
	1.45(1)	1.495(9)	1.49(1)	1.518(9)

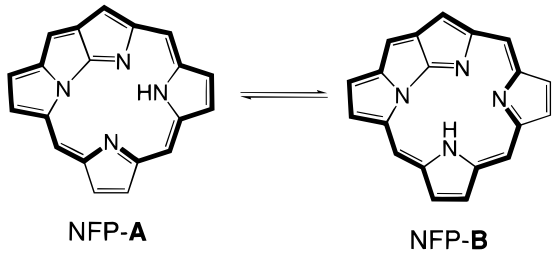

Figure 5. NH tautomers of NFP-**A** and NFP-**B**.

Table 3. Calculated Total Energies of NFP Cores for **4a**, **4b**, **4e**, **5b** and **5e**

	B3LYP/6-31G‡‡//B3LYP/3-21G (hartrees)		ΔE (kcal/mol)
	NFP-**A**	NFP-**B**	E_A-E_B
4a	−1192.798 6185	−1192.792 8129	−2.414
4b	−3559.400 3354	−3559.396 4881	−3.643
4e	−988.297 7273	−988.293 567	−2.6106
5b	−8701.602 9878	−8701.604 0795	+0.6850
5e	−6130.499 6445	−6130.501 2166	+0.9864

Structurally, two type of tautomers, NFP-**A** and NFP-**B**, can be supposed for NFPs (Figure 5). In the solid state, the preferential tautomer seems different according to the position of the substituents. Comparing the two different angles of pyrrolic N of ring-D and ring-E, NH carrying pyrrole could be assigned at D-ring (NFP-**A**) for **4a**, **4b**, and **4e**, but E-ring (NFP-**B**) for **5b** and **5e**.[15] Consistent with this, the density functional theory (DFT) calculations on the tautomers at the B3LYP/6-31G**//B3LYP/3-21G level showed the same tendency (Table 3).[16] Namely, the NFP-**A** form is 2−3 kcal/mol more stable than the NFP-**B** form for **4a**, **4b**, and **4e**, while the NFP-**B** form is ca. 1 kcal/mol more stable for **5b** and **5e**. Interestingly, the tilting angles of the D-ring against the least-squares plane for **5b** and **5e** are 27 and 23°, which are much larger than those for **4a′** and **4e′** (5−6°) (Figure 6). Such large tilts might be due to the steric repulsion between Br at C_{12} and C_{13} and ortho-hydrogens of Φ_2 and Φ_3.[17] The increase of the acidity due to the electron withdrawing substituents would also enhance the transfer of pyrrolic NH from the D-ring to E-ring.

Hydrogen Bondings of Inner NH. The observed $N_2\cdots N_3$ distances (2.469−2.558 Å) of all NFPs in the solid state are much shorter than 2.63 Å of nonsubstituted porphycene and

(15) Tülinski et al. has reported that NH carrying pyrrole has a wider $C_\alpha NC_\alpha$ angle and longer $C_\beta C_\beta$ bond length than the pyridine type of pyrrole. For example, with TPP, the $C_\alpha NC_\alpha$ bond angle of the pyrole ring carrying NH was 109.2° and the $C_\beta C_\beta$ bond length was 1.355 Å. On the other hand, the $C_\alpha NC_\alpha$ bond angle of the pyrrole ring lacking NH was 106.6°, and the $C_\beta C_\beta$ bond length was 1.341 Å. See ref 14.

(16) All calculations were performed with: *Gaussian 98W/DFT program* (Rev. A.7); Gaussian, Inc.: Pittsburgh, PA, 1998.

(17) Jaquinod, L.; Khoury, R. G.; Shen, K. M.; Smith, K. M. *Tetrahedron* **1999**, *55*, 13151−13158.

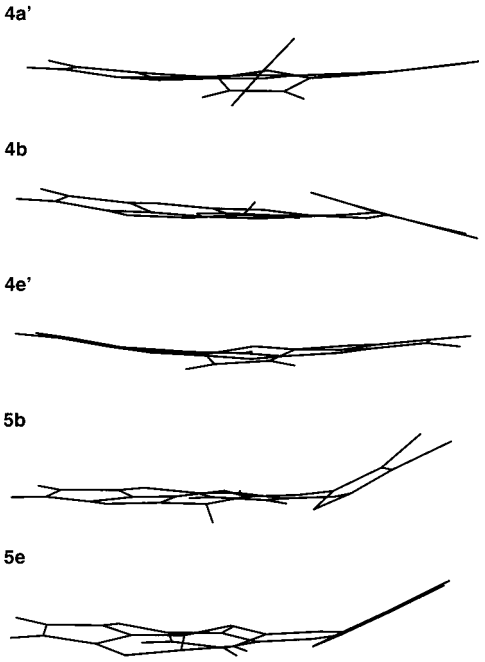

Figure 6. Side views of X-ray structure for NFPs (**4a′**, **4b**, **4e′**, **5b**, **5e**).

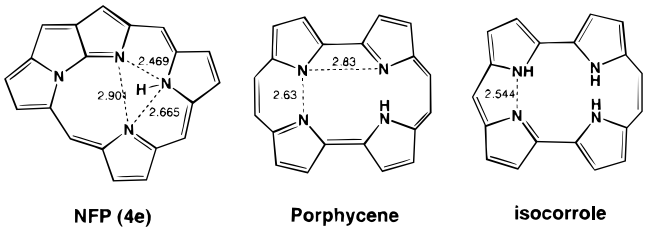

Figure 7. Comparison of bond distances and N···N distances of NFP (**4e′**) with porphycene and isocorrole.

comparable with 2.544 Å of isocorrole, in which the strong hydrogen bondings of the core NH were demonstrated (Figure 7)[18,19] The evidence of hydrogen bondings in NFPs in a $CDCl_3$ solution was obtained from unusual downfield shifts (+9 to +6 ppm) of the inner NH signals of NFPs in ^1H NMR. For example, a broad NH signal of **4e′** was observed at 8.48 ppm, in marked contrast with normal porphyrins (∼−3 ppm), and the downfield shift was more pronounced than for porphycene (3.15 ppm) and isocorrole (6.18 ppm). On the other hand, the peripheral hydrogens of the core rings were observed in the range of 9 to 7 ppm, reflecting 18π electron aromaticity. Since the splitting or shifting of the NH signal, which could be ascribed to NH tautomerism, was not observed by lowering the temperature, even at −50 °C, the hydrogen bonding involved in the NFP core seems very strong. Supporting this, the $^1H-^1H$ couplings between the inner NH and outer β-Hs of the D-ring (H_b, H_c) of **4b** were observed in C_6D_6.[20]

Since the $N_3\cdots N_4$ distances (2.63−2.74 Å) were still in the hydrogen bonding range, the three-centered (N_2, N_3, and N_4) hydrogen bonding could be considered in NFPs.[21] To confirm

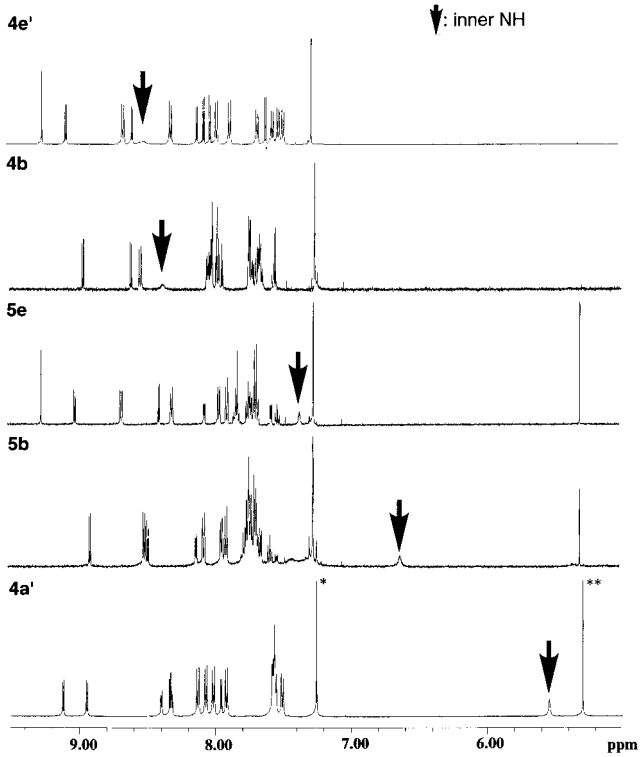

Figure 8. NH chemical shifts of NFPs (**4a′**, **4b**, **4e′**, **5b**, **5e**) in $CDCl_3$ at 27 °C: (*) $CHCl_3$; (**) CH_2Cl_2.

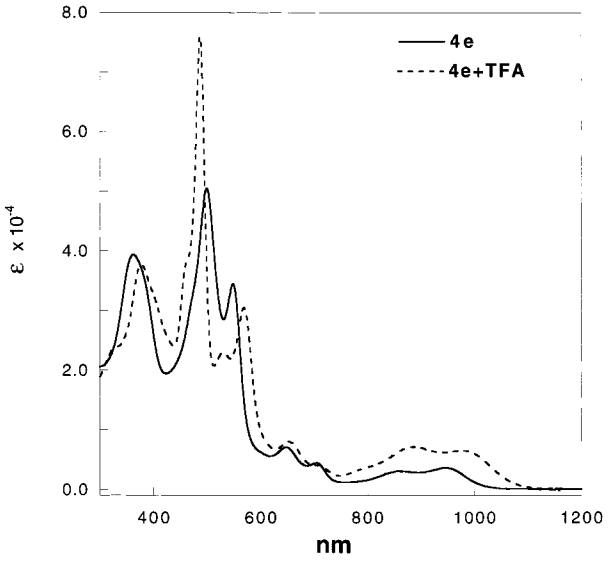

Figure 9. Absorption spectra of free base and protonated form of **4e′** in CH_2Cl_2.

this, the correlation between NH chemical shifts and N···N distances in a series of NFP derivatives as investigated. The $N_2\cdots N_4$ distances were decreased in the order of **4a′**, **4e′**, **4b**, **5e**, and **5b** (Table 1). On the other hand, the observed inner NH signals were shifted to upper field from 8.48 to 5.55 ppm in the order of **4e′**, **4b**, **5e**, **5b**, and **4a′** (Figure 8). Except in the nitro derivative **4a′**, the same trend was observed. The good accordance would be a strong indication of the formation of the three-centered hydrogen bonding among the pyrrolic three nitrogens, N_2, N_3, and N_4, in NFPs. In fact, the sum of the nitrogen distances still holds the order: $N_2\cdots N_3 + N_3\cdots N_4$ for **4e** and **4b** are 5.134 and 5.109 Å, and ($N_2\cdots N_4 + N_3\cdots N_4$) for **5e** and **5b** are 5.518 and 5.52 Å. The discrepancy of **4a′** could be explained by the higher acidity of N_2 owing to the presence

(18) (a) Vogel, E.; Köcher, M.; Scmickler, H.; Lex, J. *Angew. Chem., Int. Ed. Engl.* **1986**, *25*, 257−259. (b) Vogel, E. *J. Heterocycl. Chem.* **1996**, *33*, 1461−1487.

(19) Vogel, E.; Binsack, B.; Hellwig, Y.; Erben, C.; Heger, A.; Lex, J.; Wu, Y.-D. *Angew. Chem., Int. Ed. Engl.* **1997**, *36*, 2612−2615.

(20) To simplify the ^1H NMR spectra, *meso*-C_6D_5 derivatives of **4b** and **5b** were used for the measurements. See Supporting Information.

(21) Jeffrey, G. A.; Saenger, W. Hydrogen Bonding in Biological Structures; Springer-Verlag: Berlin, 1991; Chapter 8.

Table 4. Absorption Spectra of NFP Derivatives in CH_2Cl_2

	λ_{max} (nm) ($\log_{10} \epsilon$)						
4a′	384.0 (4.54)	522.0 (4.82)	553.0 (4.70)	656.0 (3.94)	701.0 (3.89)	841.0 (3.53)	—
4b	368.0 (4.63)	500.0 (4.70)	542.0 (4.67)	646.0 (3.85)	699.0 (3.63)	868.0 (3.47)	957.0 (3.46)
4c	366.0 (4.65)	501.0 (4.71)	544.0 (4.66)	647.0 (3.85)	701.0 (3.63)	881.0 (3.47)	964.0 (3.48)
4e′	359.0 (3.53)	499.0 (4.70)	545.0 (4.54)	648.0 (3.81)	705.0 (3.63)	855.0 (3.46)	941.0 (3.53)
4e′ + TFA	378.0 (4.58)	487.0 (4.88)	530.0/569.0 (4.36)/(3.48)	653.0 (3.90)	714.0 (3.58)	889.0 (3.85)	975.0 (3.81)
5b	381.0 (4.67)	506.0 (4.65)	565.0 (4.36)	647.0 (3.93)	701.0 (3.64)	883.0 (3.64)	969.0 (3.57)
5e	374.0 (4.65)	500.0 (4.70)	565.0 (4.29)	646.0 (3.88)	704.0 (3.69)	853.0 (3.67)	932.0 (3.67)

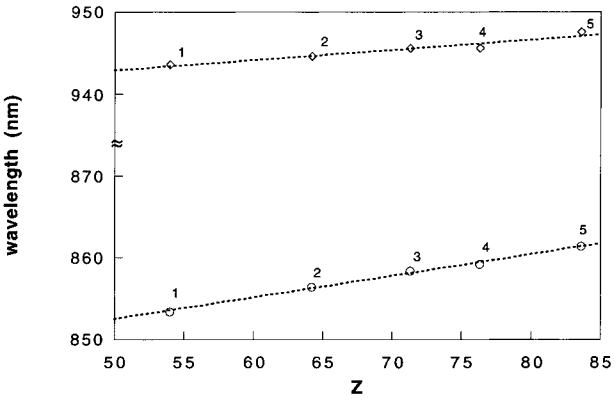

Figure 10. Plot of absorption maxima (λ_{max}) of **4e′** and Kosower's *Z* parameters: (1) Benzene ($Z = 54.0$); (2) CH_2Cl_2 ($Z = 64.2$); (3) CH_3CN ($Z = 71.3$); (4) ^{i}PrOH ($Z = 76.3$); (5) MeOH ($Z = 83.6$).

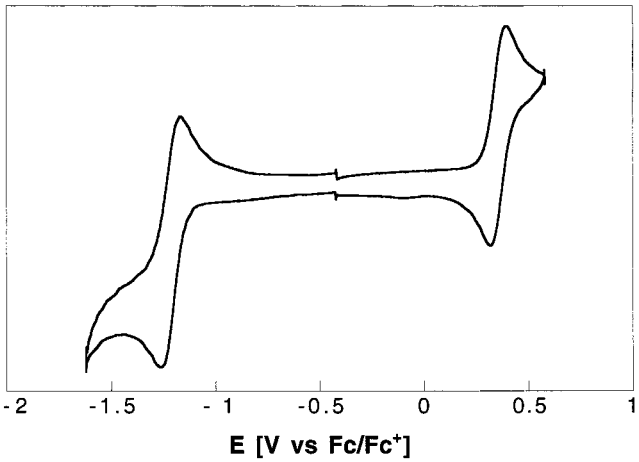

Figure 11. Cyclic voltammogram of **5b** in CH_2Cl_2, 0.1 M $(TBA)BF_4$, 100 mV/s, Pt working electrode.

of NO_2, a strong electron withdrawing group.[22] The IR spectra of NFPs are noteworthy insofar as they exhibit no typical N−H stretching vibration, which is similar to porphycenes.[18a]

Optical Spectra of NFP. The NFPs obtained exhibit Soret-like transitions around 360, 500, and 550 nm and weak Q-like bands around 650, 700, 850, and 940 nm in CH_2Cl_2. The absorption spectra of **4e′** and its protonated form are shown in Figure 9. In the presence of trifluoroacetic acid (TFA), the second Soret transition at 499.0 nm was shifted to 487.0 nm with increasing intensity. On the contrary, the near-infrared transition was shifted to longer wavelength, 975.0 nm, and the absorption edge was extended up to 1100 nm. Similar spectra were recorded with other substituted NFPs, and the characteristic long-wavelength transitions were observed in the range between 930 and 970 nm. In Table 4, λ_{max} and log ϵ for **4a′**, **4b**, **4c**, **4e′**, **5b**, and **5e** are summarized.[23]

As for the nature of the long-wavelength absorption, a possibility of the intramolecular charge transfer (CT) was examined. In Figure 10, the two absorption λ_{max} of **4e′** in the near-infrared region were plotted against Kosower's *Z*.[24] By increasing the solvent polarity, the absorption bands were shifted to the red. However, the changes were within 10 nm, and a good linear correlation was only observed in **4b**, **4c**, and **4e′**. Thus we suppose that the CT contribution to the long-wavelength transitions is small or negligible. From the electrochemical measurements, both energy levels, LUMO and HOMO seem to be perturbed. The LUMO level was lowered while the HOMO level was more significantly raised (vide infra) relative to TPP. The PM3 calculation showed the localization of spin density at the tri-pentacyclic ring, both at HOMO and LUMO levels.[25] Reflecting that the introduction of a substituent directly at the tri-pentacyclic ring caused the optical absorption change largely compared to the other pyrrolic position. In fact, in the case of **4a′**, the absorption at the longest wavelength near 1000 nm was diminished due to the strong resonance effect of the nitro group.

Electrochemical Measurements for NFPs. The first oxidation and reduction potential for NFP derivatives (**4a′**, **4b**, **4c**, **4e′**, **5b**, and **5e**) were determined by the cyclic voltammetry (CV). As a typical example, the CV spectrum of **5b** is shown in Figure 11. The second oxidation and reduction were irreversible and could not be explicitly determined with all NFPs examined. The electrochemical data are summarized in Table 5. In comparison with TPP, the electrode oxidation process of **4e′** was shifted 0.48 V to negative potentials; on the other hand, E_{red} was shifted only 0.11 V in the opposite direction.[26] Therefore, the small energy gap attributed to the long-

(22) By the ab initio calculations the electron withdrawing substituents of a hydrogen acceptor molecule were shown to weaken the hydrogen bondings ability. See: (a) Del Bene, J. E.; Person, W. B.; Szczepaniak, K. *Chem. Phys. Lett.* **1995**, *247*, 89−94. (b) Del Bene, J. E.; Person, W. B.; Szczepaniak, K. *Mol. Phys.* **1996**, *89*, 47−59.

(23) The UV/vis spectra for **4a′**, **4b**, **4c**, **5b**, and **5e** are shown in Supporting Information.

(24) Reichardt, C. *Solvent Effects in Organic Chemistry*; Verlag Chemie: Weinheim, Germany, 1978; p 237.

(25) Calculation was performed using: *WinMOPAC program*, version 2.0; Fujitsu: Tokyo, 1998. HOMO and LUMO orbitals of NFP are shown in Supporting Information.

(26) Rao, T.; Maiya, B. G. *Polyhedron*. **1994**, *13*, 1863−1873.

Table 5. First Oxidation and Reduction Potentials of NFPs (volt vs Fc/Fc^+, 0.1 M Bu_4NBF_4)

	E_{Ox1} (V)	E_{Red1} (V)	$\lvert E_{Ox1} - E_{Red1}\rvert$	λ_{max} (nm)
4a′	0.48	−1.14	1.62	
4b	0.28	−1.32	1.60	957.0
4c	0.27	−1.29	1.56	964.0
4e′	0.08	−1.37	1.45	941.0
5b	0.36	−1.20	1.56	969.0
5e	0.21	−1.27	1.48	932.0
TPP[a]	0.56	−1.48	2.04	647.0

[a] Ref 26.

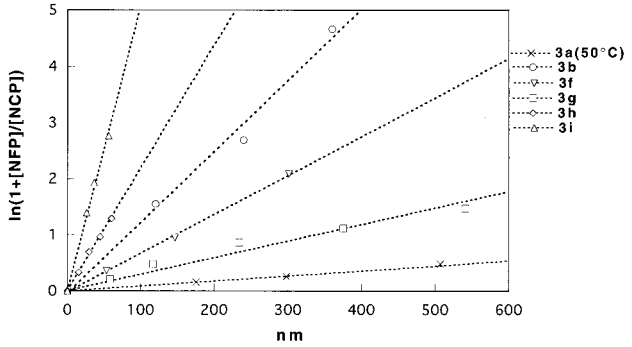

Figure 12. Time course of NFP formation for **3b**, **3f**, **3g**, **3h**, and **3i** at 30 °C (**3a**: at 50 °C).

Scheme 4

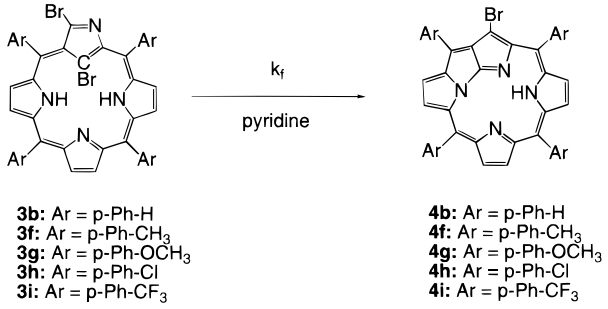

wavelength transitions was caused mainly by the raised HOMO level.

Mechanistic Study of NFP Formation. The reaction of NFP formation was largely affected on the substituents, both at the *meso*-position and the inner carbon. To investigate the mechanism in details, the time course of NFP formation for a series of dibrominated NCPs (phenyl (**3b**), *p*-tolyl (**3f**), *p*-anisyl (**3g**), *p*-chlorophenyl (**3h**), and *p*-trifluoromethylphenyl (**3i**)) were followed (Figure 12). Apparently, the introduction of the electron withdrawing groups accelerated the reaction. A series of the first-order rate constants (k_f) obtained at 30 °C differ largely ($k_{f-3i}/k_{f-3g} = 17$), and the good correlation with Hammet σ^+, indicates the intervening of the π-resonance effect in the transition state (Scheme 4, Figure 13).[27] The obtained thermodynamic parameters are summarized in Table 6. In the fastest case, **3i**, both entropy and enthalpy gains were manifested in comparison with the slowest case, **3g**. With the electron withdrawing substituents, the intervening of the tautomeric form NCP-**B** (Scheme 5) was suggested from the ^1H NMR measurement of **2b**.[28] Such a tautomer is inferred to be less aromatic

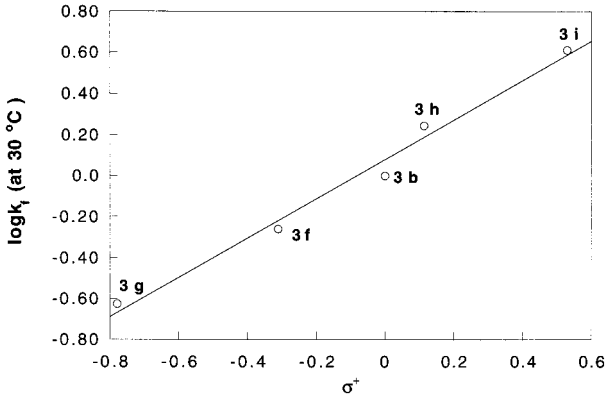

Figure 13. Hammet (σ^+) plot against log k_f for NFP formation (at 30 °C).

Table 6. Thermodynamic Parameters of NFP Formation for **3a′**, **3b**, **3f**, **3g**, **3h**, and **3i**

	E_A (kcal/mol)	$\Delta G_f^{\ddagger}$ (300 K, kcal/mol)	$\Delta H_f^{\ddagger}$ (kcal/mol)	$\Delta S_f^{\ddagger}$ (cal/mol·K)
3a′	22.4	25.8	21.8	−13.3
3b	14.8	22.6	14.2	−28.0
3f	21.4	23.1	20.9	−7.3
3g	23.5	23.8	22.9	−3.0
3h	19.0	22.5	18.4	−13.7
3i	12.3	21.9	11.7	−34.0

[a] E_A: Arrhenius activaion energy.

Scheme 5

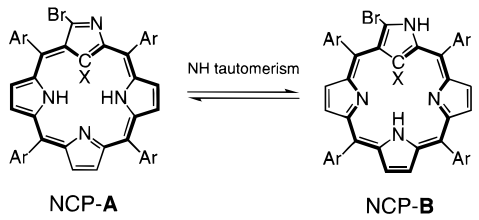

and could show the conformational flexibility, resulting in the facile inversion of the confused pyrrole ring.[29] On the other hand, the replacement of the inner C−Br to C−NO_2 (**3a**) showed slow NFP formation, which might be ascribed to the lower activity of the leaving Br group on the confused pyrrole bearing an electron withdrawing NO_2.

Reinversion to NCP. Interestingly, the NFPs obtained were transformed again into NCP. When **4b** was treated with MeONa/MeOH in CH_2Cl_2 for 30 min, the red color solution gradually changed to green and, surprisingly, methoxy-substituted NCP, **6a**, was formed in 72% yield (Scheme 6). When the reaction mixture was stirred longer, the debrominated product **6b** was detected. The same type of reaction was also observed with other NFPs. That might be triggered by the disappearance of hydrogen bonding due to the deprotonation by the base added. The successive nucleophilic attack at the bridged C_9 position of **4b** by MeO^- might be an initiation of the ring opening and rebirth of the confused pyrrole ring. To support this, when nucleophile other than MeO^-, such as OH^-, was present, the oxo-substituted amide NCP, a stable tautomer of hydroxy-substituted NCP, **6d**, was obtained. Therefore, the ring opening reaction of NFPs would constitute a useful synthetic pathway to prepare the various NCP derivatives.

(27) (a) Brown, H. C.; Okamoto, Y. *J. Am. Chem. Soc.* **1957**, *79*, 1913−1917. (b) Brown, H. C.; Okamoto, Y. *J. Am. Chem. Soc.* **1958**, *80*, 4979−4987. (c) Swain, C. G.; Unger, S. H.; Rosenquist, N. R.; Swain, M. S. *J. Am. Chem. Soc.* **1983**, *105*, 492−502. (d) Hansch, C.; Leo, A.; Taft, R. W. *Chem. Rev.* **1991**, *91*, 165−195.

(28) For **2b**, the outer NH signal at 10.96 ppm, which belongs to the tautomer NCP-**B**, was observed in DMF-d_7 at room temperature.

(29) NMR and UV/vis changes of the NH tautomer of NCPs were reported: Japanese Chemical Society, annual meeting, 1998, March, Kyoto, Japan. Full accounts of the NH tautomerism for NCPs will be reported in due course.

Scheme 6

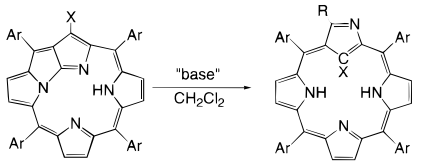

(Ar = Ph or p-tolyl)

6a: X =Br, R = OMe
6b: X = H, R = OMe
6c: X = H, R = OEt
6d: X = H, R = OH
6e: X = NO_2, R = OMe

Conclusions

The halide-substituted NCPs were transformed into a novel 18π aromatic porphyrinoid with a fused tri-pentacyclic ring in the core, NFPs. NFPs show the unusual long-wavelength absorption and the strong hydrogen bondings between inner nitrogens. The planarity of the structures was confirmed by X-ray analyses. The NFPs formation reaction was accelerated by the electron withdrawing substituents at the meso positions. Further, the reverse reaction from NFPs to NCPs could take place in the presence of base. Such reversibility associated with a color change might be potentially useful for optical applications. Furthermore, the low-energy band gap of NFP would be of interest for use as conductive materials as well.

Experimental Section

General Methods. Commercially available solvents and reagents were used without further purification unless otherwise mentioned. NBS was recrystallized from water, and dichloromethane was distilled from P_2O_5. NCPs were synthesized from freshly distilled aryl aldehydes, and pyrrole was by the reported procedure.[7a] Thin-layer chromatography (TLC) was carried out on aluminum sheets coated with silica gel 60 (Merck 5554). UV−visible spectra were recorded on a Shimadzu UV-2400 spectrometer and a Shimadzu UV-3100PC spectrometer. ^{1}H NMR and ^{13}C NMR spectra were recorded on a JEOL α-500 spectrometer (operating at 500.00 MHz for ^{1}H and 125.65 MHz for ^{13}C) using the deuterated chloroform as the internal lock and the residual solvent as the internal reference. Fast atom bombardment mass spectra (FAB-MS) were recorded on a JEOL-HX110 in the positive ion mode with a xenon primary atom beam with a 3-nitrobenzyl alcohol matrix. Cyclic and differential pulse voltammetric measurements were performed with a CH Instrument Model 660 using a Pt electrode. Elemental analyses were performed by the Elemental Analysis Center of Kyoto University

N-Confused Tetraphenylporphyrin-(Br, H), 2b. To a CH_2Cl_2 solution of NCTPP (**1**) (16.73 mg, 0.0272 mmol) was added NBS (4.97 mg 0.0279 mmol), and this was stirred for 5 min. After evaporation, the residues were separated by a silica gel column with CH_2Cl_2. The first green fraction gave **2b** (16.8 mg, 0.0242 mmol) in 89% yield. ^{1}H NMR: δ 7.23 (s, 1H), 7.80 (m, 16H), 8.15 (m, 4H), 8.43 (m, 3H), 8.50 (m, 2H), 8.57 (d, 1H, J = 4.5 Hz), 8.92 (d, 1H, J = 4.5 Hz), 9.02 (d, 1H, J = 5.0 Hz). UV/vis (CH_2Cl_2, λ_{max} (log ϵ)): 737.0 (4.15), 680.0 (3.54), 595.0 (4.05), 552.0 (4.02), 453.0 (5.15). FAB-MS: m/z = 692.7 (calcd for $C_{44}H_{29}N_4Br$ [M^+] 692.1576).

N-Confused Tetraphenylporphyrin-(Cl, H), 2c. To a CH_2Cl_2 solution of **1** (30.7 mg, 0.0501 mmol) was added NCS (6.70 mg 0.0511 mmol), and this was stirred for 5 min. After evaporation, the residues were separated by a silica gel column with CH_2Cl_2. The first green fraction gave **2c** (30.4 mg, 0.0475 mmol) in 94% yield. ^{1}H NMR: δ 7.78 (m, 16H), 8.01 (d, 1H, J = 7.0 Hz), 8.16, (m, 2H), 8.24 (m, 1H), 8.43 (m, 3H), 8.51 (m, 3H), 8.57 (d, 1H, J = 5.0 Hz). UV/vis (CH_2Cl_2, λ_{max}): 734.0, 670.0, 591.5, 548.5, 449.5. FAB-MS: m/z = 648.7 (calcd for $C_{44}H_{29}N_4Cl$ [M^+] 648.2159).

N-Confused Tetratolylporphyrin-(NO_2, Br), 3a′. To a CH_2Cl_2 solution of **2a′** (51.08 mg, 0.0714 mmol) was added NBS (13.79 mg 0.0775 mmol), and this was stirred for 5 min. After evaporation, the residues were separated by a silica gel column with CH_2Cl_2. The first dark yellow fraction gave **3a′** (54.1 mg, 0.0682 mmol) in 96% yield. ^{1}H NMR: δ 2.73 (m, 12H), 7.56 (m, 5H), 7.74 (m, 5H), 7.92 (d, 1H, J = 7.5 Hz), 8.02 (d, 2H, J = 8.0 Hz), 8.15 (d, 1H, J = 7.5 Hz), 8.38 (m, 4H), 8.49 (m, 2H), 8.69 (d, 2H, J = 4.5 Hz), 9.12 (d, 1H, J = 4.5 Hz), 9.18 (d, 1H, J = 4.5 Hz). UV/vis (CH_2Cl_2, λ_{max}): 728.5, 664.0, 612.0, 487.0, 383.0. FAB-MS: m/z = 794.2 (calcd for $C_{48}H_{36}N_5OBr$ [M^+ + H] 794.2131).

N-Confused Tetraphenylporphyrin-(Br, Br), 3b. To a CH_2Cl_2 solution of **1** (11.90 mg, 0.0194 mmol) was added NBS (7.98 mg 0.0448 mmol), and this was stirred for 5 min. After evaporation, the residues were separated by the silica gel column with CH_2Cl_2. The second green fraction gave **3b** (11.8 mg, 0.0153 mmol) in 79% yield. ^{1}H NMR: δ 7.81 (m, 14H), 8.01 (d, 2H, J = 7.5 Hz), 8.10 (m, 1H), 8.25 (d, 1H, J = 6.5 Hz), 8.38 (m,4H), 8.43 (m, 2H), 8.45 (d, 1H, J = 5.0 Hz), 8.80 (d, 1H, J = 5.0 Hz), 8.94 (d, 1H, J = 5.0 Hz). UV/vis (CH_2Cl_2, λ_{max} (log ϵ)): 757.0 (4.15), 698.0 (3.63), 606.0 (3.74), 563.0 (4.01), 465.0 (5.11). FAB-MS: m/z = 771.3 (calcd for $C_{44}H_{29}N_4Br_2$ [M^+ + H] 771.0760).

N-Confused Tetraphenylporphyrin-(Cl, Br), 3c. To a CH_2Cl_2 solution of **2c** (17.8 mg, 0.0278 mmol) was added NBS (5.76 mg 0.0324 mmol), and this was stirred for 5 min. After evaporation, the residues were separated by a silica gel column with CH_2Cl_2. The second dark yellow fraction gave **3c** (13.3 mg, 0.0183 mmol) in 66% yield. ^{1}H NMR: δ 7.80 (m, 14H), 8.01 (d, 1H, J = 7.0 Hz), 8.10 (m, 2H), 8.27 (d, 1H, J = 7.0 Hz), 8.33 (d, 1H, J = 4.5 Hz), 8.36 (d, 1H, J = 4.5 Hz), 8.39 (d, 1H, J = 5.5 Hz), 8.42 (m, 5H), 8.77 (d, 1H, J = 4.5 Hz), 8.91 (d, 1H, J = 5.5 Hz). UV/vis (CH_2Cl_2, λ_{max}): 760.5, 665.0, 607.0, 565.0, 466.5. FAB-MS: m/z = 726.6 (calcd for $C_{44}H_{29}N_4ClBr$ [M^+ + H] 727.1218).

N-Fused Tetratolylporphyrin-(NO_2, H), 4a′. A pyridine solution of **3a′** (54.1 mg, 0.0682 mmol) was stirred for 3 h at 80 °C. After evaporation, the residues were separated by a silica gel column with CH_2Cl_2. The third red fraction collected gave **4a′** (45.8 mg, 0.0682 mmol) in 94% yield. ^{1}H NMR: δ 2.64 (m, 12H), 5.55 (s, 1H), 7.51 (d, 2H, J = 7.5 Hz), 7.57 (m, 6H), 7.93 (d, 2H, J = 8.0 Hz), 7.97 (d, 1H, J = 5.0 Hz), 8.02 (d, 2H, J = 8.0 Hz), 8.08 (d, 2H, J = 8.0 Hz), 8.14 (d, 2H, J = 8.0 Hz), 8.34 (m, 2H), 8.41 (d, 1H, J = 4.5 Hz), 8.95 (d, 1H, J = 5.0 Hz), 9.12 (d, 1H, J = 5.0 Hz). ^{13}C NMR: δ 21.43, 21.51, 21.54, 21.63, 117.47, 120.30, 121.95, 123.05, 127.34, 127.47, 128.75, 128.91, 129.12, 129.38, 130.34, 130.59, 131.35, 131.92, 132.90, 132.98, 133.22, 133.47, 135.07, 135.91, 136.23, 137.72, 137.87, 138.39, 138.64, 138.64, 138.91, 141.97, 142.32, 143.08, 144.95, 147.88, 149.28, 155.16, 155.72. UV/vis (CH_2Cl_2, λ_{max} (log ϵ)): 841.0 (3.53), 701.0 (3.89), 656.0 (3.94), 553.0 (4.70), 522.0 (4.82), 384.0 (4.54). HRMS (FAB). Calcd for $C_{48}H_{36}N_5O_2$ [M^+ + H]: 714.2869. Found: 714.2824. Anal. Calcd for $C_{48}H_{37}N_5O_3$ [M + H_2O]: C, 78.78; H, 5.10; N, 9.57. Found: C, 78.34; H, 4.78; N, 9.21.

N-Fused Tetraphenylporphyrin-(Br, H), 4b. A pyridine solution of **3b** (65.7 mg, 0.0853 mmol) was stirred for 8 h at room temperature. After evaporation, the residues were separated by a silica gel column with CH_2Cl_2. The third red fraction collected gave **4b** (51.3 mg, 0.0742 mmol) in 87% yield. ^{1}H NMR: δ 7.55 (d, 1H, J = 4.5 Hz), 7.56 (t, 1H, J = 4.0 Hz), 7.70 (m, 11H), 7.94 (d, 1H, J = 4.5 Hz), 7.97 (m, 2H), 7.99 (m, 2H), 8.04 (m, 4H), 8.38 (s, 1H), 8.54 (dd, 2H, J = 1.5, 7.0 Hz), 8.61 (d, 1H, J = 5.0 Hz), 8.96 (d, 1H, J = 5.0 Hz). ^{13}C NMR: δ 95.89, 114.44, 119.30, 119.93, 124.60, 125.45, 127.04, 127.61, 127.72, 127.74, 127.83, 128.22, 128.38, 128.90, 129.04, 130.13, 132.02, 132.52, 132.98, 133.10, 133.37, 133.74, 134.08, 134.45, 136.83, 137.16, 138.96, 139.34, 141.68, 145.47, 146.23, 146.59, 150.45, 154.45, 154.43, 157.91. UV/vis (CH_2Cl_2, λ_{max} (log ϵ)): 957.0 (3.46), 868.0 (3.46), 699.0 (3.63), 646.0 (3.85), 542.0 (4.67), 500.0 (4.69), 368.0 (4.63). HRMS (FAB). Calcd for $C_{44}H_{28}N_4Br$ [M^+ + H]: 691.1511. Found: 691.1519. Anal. Calcd for $C_{44}H_{27}N_4Br$: C, 76.41; H, 3.93; N, 8.10; Br, 11.55. Found: C, 76.51; H, 3.77; N, 7.90; Br, 11.58.

N-Fused Tetraphenylporphyrin-(Cl, H), 4c. A pyridine solution of **3c** (13.3 mg, 0.0181 mmol) was stirred for 8 h at room temperature. After evaporation, the residues were separated by a silica gel column with CH_2Cl_2. The third red fraction collected gave **4c** (10.5 mg, 0.0162 mmol) in 89% yield. ^{1}H NMR: δ 7.51 (d, 1H, J = 4.5 Hz), 7.54 (t, 1H, J = 7.5 Hz), 7.70 (m, 10H), 7.91 (d, 1H, J = 4.5 Hz), 7.95 (m, 9H), 8.56 (d, 1H, J = 5.5 Hz), 8.58 (d, 2H, J = 7.0 Hz), 8.69 (s, 1H).

^{13}C NMR: δ 119.25, 119.96, 125.52, 125.29, 125.90, 127.08, 127.58, 127.74, 127.84, 128.24, 128.85, 129.25, 130.38, 131.90, 132.01, 132.82, 132.97, 133.33, 134.01, 134.08, 134.33, 134.72, 136.74, 137.13, 138.92, 139.39, 141.60, 144.52, 146.18, 149.74, 154.32. UV/vis (CH_2Cl_2, λ_{max} (log ϵ)): 964.0 (3.48), 881.0 (3.47), 701.0 (3.63), 647.0 (3.85), 544.0 (4.66), 501.0 (4.71), 366.0 (4.65). HR-MS (FAB). Calcd for $C_{44}H_{27}N_4Cl$ [$M^+ + H$]: 647.2002. Found: 647.2075.

N-Fused Tetraphenylporphyrin-(H, H), 4e. A pyridine solution of **4b** (20.21 mg, 0.0292 mmol) was refluxed for 12 h. After evaporation, the residues were separated by a silica gel column with CH_2Cl_2. The first red fraction gave recovered **4b** (10.0 mg, 0.0145 mmol, 50%) and the second red fraction afforded **4e** (7.91 mg, 0.0129 mmol) in 44% yield. ^{1}H NMR (27 °C): δ 7.51 (t, 1H, 5 Hz), 7.56 (d, 1H, J = 4.0 Hz), 7.75 (m, 11H), 8.02 (m, 6H), 8.11 (d, 1H, J = 5.0 Hz), 8.75 (d, 2H, J = 7.5 Hz), 9.11 (d, 1H, J = 5.0 Hz), 9.24 (s, 1H). ^{1}H NMR (−60 °C): δ 7.55 (m, 2H), 7.80 (m, 12H), 7.98 (d, 2H, J = 7.5 Hz), 8.08 (m, 3H), 8.17 (m, 1H), 8.34 (s, 1H), 8.44 (d, 2H, J = 7.0 Hz), 8.59 (d, 1H, J = 5.0 Hz), 8.79 (d, 2H, J = 7.5 Hz), 9.16 (d, 1H, J = 5.0 Hz), 9.33 (s, 1H). ^{13}C NMR: δ 111.50, 117.23, 120.85, 123.63, 124.28, 127.21, 127.98, 128.01, 128.44, 128.80, 128.85, 129.51, 129.74, 129.81, 130.18, 130.79, 131.65, 132.36, 133.18, 133.30, 133.34, 133.67, 134.86, 135.32, 136.85, 137.28, 138.18, 138.66, 140.34, 146.17, 151.70, 152.99. UV/vis (CH_2Cl_2, λ_{max}): 941.0, 858.0, 702.0, 648.0, 549.0, 499.0, 363.0. HR-MS (FAB). Calcd for $C_{44}H_{28}N_4$: 613.2392. Found: 613.2483. Anal. Calcd for $C_{44}H_{28}N_4$: C, 86.25; H, 4.61; N, 9.14. Found: C, 86.54; H, 4.28; N, 9.17.

N-Fused Tetratolylporphyrin-(H, H), 4e′. ^{1}H NMR: δ 2.63 (m, 12H), 7.47 (d, 2H, J = 7.5 Hz), 7.50 (d, 2H, J = 8.0 Hz), 7.55 (d, 2H, J = 8.0 Hz), 7.60 (d, 1H, J = 4.0 Hz), 7.66 (d, 2H, J = 8.0 Hz), 7.86 (d, 2H, J = 8.0 Hz), 7.96 (d, 2H, J = 7.5 Hz), 8.05 (d, 1H, J = 4.5 Hz), 8.10 (d, 1H, J = 4.5 Hz), 8.29 (d, 2H, J = 8.0 Hz), 8.48 (s, 1H), 8.57 (d, 1H, J = 5.0 Hz), 8.64 (d, 2H, J = 8.0 Hz), 9.06 (d, 1H, J = 5.0 Hz), 9.23 (s, 1H). ^{13}C NMR: δ 21.47, 21.49, 21.50, 21.52, 109.99, 113.20, 118.38, 119.53, 124.60, 124.84, 127.61, 128.48, 129.19, 129.37, 130.15, 130.37, 130.41, 131.30, 132.43, 132.98, 133.04, 133.25, 133.89, 133.95, 134.23, 135.85, 136.46, 136.50, 137.19, 137.83, 138.03, 138.97, 140.08, 142.11, 143.51, 145.55, 151.50, 152.57, 152.65, 156.05. UV/vis (CH_2Cl_2, λ_{max} (log ϵ)): 941.0 (3.53), 855.0 (3.46), 705.0 (3.63), 648.0 (3.81), 545.0 (4.54), 499.0 (4.70), 359.0 (4.62). UV/vis (CH_2Cl_2 + 15% TFA, λ_{max} (log ϵ)): 975.0 (3.81), 889.0 (3.85), 714.0 (3.58), 653.0 (3.90), 569.0 (4.48), 530.0 (4.36), 487.0 (4.88), 378.0 (4.58). HR-MS (FAB). Calcd for $C_{48}H_{37}N_4$ [$M^+ + H$]: 669.3018. Found: 669.3110.

N-Fused Tetraphenylporphyrin-(Br, Br$_2$), 5b. To a pyridine solution of **4b** (6.64 mg, 0.0096 mmol) was added NBS (3.64 mg, 0.0205 mmol), and this was stirred for 5 min at room temperature. After evaporation, the residues were separated by a silica gel column with CH_2Cl_2. The first red fraction collected gave **5b** (8.0 mg, 0.0094 mmol) in 98% yield. ^{1}H NMR: δ 6.68 (s, 1H), 7.59 (m, 1H), 7.73 (m, 12H), 7.93 (m, 4H), 8.06 (m, 2H), 8.12 (d, 1H, J = 5.0 Hz), 8.50 (d, 1H, J = 5.0 Hz), 8.51 (m, 2H), 8.95 (d, 1H, J = 5.0 Hz). ^{13}C NMR: δ 100.38, 113.67, 115.83, 117.38, 119.57, 121.62, 127.89, 128.19, 128.30, 128.64, 129.28, 129.48, 129.71, 129.83, 130.13, 130.21, 131.40, 132.33, 132.95, 133.33, 133.55, 134.02, 134.49, 134.56, 136.82, 137.56, 138.33, 140.56, 141.84, 144.60, 144.69, 145.69, 146.47, 147.83, 149.46, 151.81. UV/vis (CH_2Cl_2, λ_{max} (log ϵ)): 969.0 (3.57), 883.0 (3.64), 701.0 (3.64), 647.0 (3.93), 565.0 (4.36), 506.0 (4.65), 381.0 (4.67). HR-MS (FAB). Calcd for $C_{44}H_{26}N_4Br_3$ [$M^+ + H$]: 846.9708. Found: 846.9730. Anal. Calcd for $C_{44}H_{25}N_4Br_3$: C, 62.86; H, 2.97; N, 6.60; Br, 28.22. Found: C, 62.22; H, 2.97; N, 6.60; Br, 28.76.

N-Fused Tetraphenylporphyrin-(H, Br$_2$), 5e. A pyridine solution of **5b** (48.4 mg, 0.0570 mmol) was refluxed for 12 h. After evaporation, the residues were separated by a silica gel column. The first red fraction gave the recovered **5b** (16.4 mg, 0.0193 mmol, 34%) and the second red fraction afforded **5e** (21.6 mg, 0.0281 mmol) in 49% yield. ^{1}H NMR: δ 7.36 (s, 1H), 7.52 (t, 1H, J = 7.3 Hz), 7.57 (dd, 1H, J = 4.5 Hz, 1.5 Hz), 7.70 (m, 8H), 7.83 (m, 3H), 7.93 (m, 4H), 8.06 (dd, 1H, J = 5.0 Hz, 1.0 Hz), 8.30 (dd, 2H, J = 8.0 Hz, 1.5 Hz), 8.40 (d, 1H, J = 5.0 Hz), 8.67 (d, 2H, J = 8.0 Hz), 9.01 (d, 1H, J = 4.5 Hz), 9.26 (s, 1H). ^{13}C NMR: δ 113.02, 113.91, 114.30, 115.78, 118.28, 120.85, 127.49, 127.80, 128.14, 128.25, 128.54, 129.08, 129.14, 129.28, 129.40, 129.44, 129.75, 130.06, 132.95, 133.82, 134.34, 134.65, 135.21, 135.99, 138.11, 138.72, 139.45, 140.61, 143.45, 144.32, 145.42, 145.76, 150.57, 153.20, 155.04. UV/vis (CH_2Cl_2, λ_{max} (log ϵ)): 932.0 (3.67), 853.0 (3.67), 704.0 (3.69), 646.0 (3.88), 565.0 (4.29), 500.0 (4.70), 374.0 (4.65). HR-MS (FAB). Calcd for $C_{44}H_{27}N_4Br$ [$M^+ + H$]: 771.0587. Found: 771.0577. Anal. Calcd for $C_{44}H_{26}N_4Br_2$: C, 68.59; H, 3.40; N, 7.27; Br, 20.74. Found: C, 68.39; H, 3.31; N, 7.04; Br, 20.63.

N-Confused Tetraphenylporphyrin-(Br, OMe), 6a. To a CH_2Cl_2 solution of **4b** (7.30 mg, 0.011 mmol) was added NaOMe (28% solution in MeOH), and this was stirred overnight. After neutralizing with 5% HCl, dried over $NaSO_4$, the solvent was evaporated. The resulting residues were separated by a silica gel column with 1% MeOH/CH_2Cl_2. The second yellow-green fraction afforded a trace amount of purple solid, **6a** (5.7 mg, 0.00786 mmol) in 71.5% yield. Compound **6a** was found unstable and was transformed to the debrominated product, **6b**, during the reaction. ^{1}H NMR: δ 3.57 (s, 3H), 7.76 (m, 12H), 8.02 (m, 2H), 8.18 (m, 2H), 8.33 (m, 3H), 8.43 (m, 5H), 8.66 (d, 1H, J = 4.5 Hz), 8.82 (d, 1H, J = 4.5 Hz). UV/vis (CH_2Cl_2, λ_{max}): 720.5, 604.5, 560.5, 460.0. FAB-MS: m/z = 722.4 (calcd for $C_{45}H_{31}N_4OBr$ [M^+] 722.1681).

N-Confused Tetraphenylporphyrin-(H, OMe), 6b. To a CH_2Cl_2 solution of **4b** (12.43 mg, 0.018 mmol) was added NaOMe (28% solution in MeOH) and this was stirred for 24 h. After neutralizing with 5% HCl, dried over Na_2SO_4, the solvent was evaporated. The resulting residues were separated by a silica gel column with 1% MeOH/CH_2Cl_2. The first yellow-green fraction gave **6b** (5.05 mg, 0.0078 mmol) in 45% yield. ^{1}H NMR: δ −5.09 (s, 1H), 4.01 (s, 3H), 7.74 (m, 12H), 8.16 (m, 6H), 8.38 (m, 2H), 8.45 (d, 1H, J = 4.5 Hz), 8.50 (d, 1H, J = 4.5 Hz), 8.52 (d, 1H, J = 4.5 Hz), 8.55 (d, 1H, J = 4.5 Hz), 8.72 (d, 1H, J = 4.5 Hz), 8.73 (d, 1H, J = 4.5 Hz). UV/vis (CH_2Cl_2, λ_{max}): 706.5, 640.0, 588.0, 544.0, 442.0. FAB-MS: m/z = 645.1 (calcd for $C_{45}H_{33}N_4O$ [$M^+ + H$] 645.2654).

N-Confused Tetraphenylporphyrin-(H, OEt), 6c. To a CH_2Cl_2 (10 mL) solution of **4b** (13.20 mg, 0.0191 mmol) was added 150 μL of EtOH solution containing the saturated NaOEt. The solution was stirred for 18 h and then washed with 5% HCl(aq). After drying over Na_2SO_4, the solvent was evaporated. The resulting residues were separated with a silica gel column. The first green fraction collected gave **6c** (8.62 mg, 0.0134 mmol) in 71% yield. ^{1}H NMR: δ −5.13 (s, 1H), 1.10 (t, 3H, J = 7.5 Hz), 4.55 (q, 2H, J = 7.5 Hz), 7.72 (m, 12H), 8.16 (m, 6H), 8.37 (d, 2H, J = 7.5 Hz), 8.45 (d, 1H, J = 4.5 Hz), 8.50 (d, 1H, J = 4.5 Hz), 8.53 (d, 1H, J = 5.0 Hz), 8.55 (d, 1H, J = 5.0 Hz), 8.72 (d, 1H, J = 5.0 Hz), 8.75 (d, 1H, J = 5.0 Hz). UV/vis (CH_2Cl_2, λ_{max}) 703.0, 650.0, 584.0, 541.0, 441.0. FAB-MS: m/z = 659.4 (calcd for $C_{46}H_{35}N_4O$ [$M^+ + H$] 659.2811).

N-Confused Porphyrin-(H, oxo), 6d. Compound **4b** (10.65 mg, 0.0154 mmol) was solved to CH_2Cl_2 (20 mL), and 20 M KOH(aq) 3 mL was added to the solution. And the two phases were stirred vigorously for 2 days. The organic phase was separated, washed with 5% HCl(aq), and dried over Na_2SO_4. The solvent was evaporated, and the residue was purified with a silica gel column. The first green fraction afforded **6d** (6.03 mg, 0.0096 mmol) in 62% yield. ^{1}H NMR: δ −5.37 (s, 1H), 7.53 (t, 1H, J = 7.0 Hz), 7.77 (m, 10H), 7.94 (d, 2H, J = 7.0 Hz), 8.15 (m, 5H), 8.21(m, 4H), 8.48 (s, 1H), 8.56 (m, 4H), 8.63 (d, 1H, J = 4.5 Hz), 8.73 (d, 1H, J = 5.0 Hz). ^{13}C NMR: δ 85.68, 88.59, 102.11, 111.07, 118.82, 119.03, 120.47, 124.86, 125.59, 126.33, 126.68, 126.92, 127.42, 127.77, 127.86, 128.59, 128.78, 129.08, 132.66, 133.56, 134.09, 134.16, 134.28, 134.46, 134.80, 136.61, 136.98, 137.78, 138.08,138.32, 139.32, 140.16, 141.91, 154.41, 167.10, 188.48. UV/vis (CH_2Cl_2, λ_{max}): 697.5, 633.0, 580.5, 538.0, 443.0. HR-MS (FAB). Calcd for $C_{44}H_{31}N_4O$ [$M^+ + H$]: 631.2498. Found: 631.2421.

N-Confused Tetratolylporphyrin-(NO$_2$, OMe), 6e′. To a CH_2Cl_2 (20 mL) solution of **4a′** (14.30 mg, 0.0200 mmol) was added NaOMe (28% MeOH solution, 50 μL), and the mixture was stirred for 18 h. After neutralizing with 5% HCl, dried over Na_2SO_4, the solvent was evaporated. The resulting residues were separated by a silica gel column with 1% MeOH/CH_2Cl_2. The first fraction collected afforded **6e′** (14.6 mg, 0.0196 mmol) in 98% yield. ^{1}H NMR: δ 2.68 (m, 12H), 3.77 (s, 3H), 7.59 (m, 8H), 7.93 (d, 1H, J = 7.5 Hz), 8.00 (d, 1H, J = 7.5 Hz), 8.05 (d, 1H, J = 7.5 Hz), 8.16 (d, 1H, J = 7.5 Hz), 8.21 (d, 2H, J = 7.5 Hz), 8.30 (d, 2H, J = 7.5 Hz), 8.53 (d, 1H, J = 4.5 Hz), 8.60 (d,

Table 7. Crystallographic Details for **4a′**, **4b**, **4e′**, **5b**, and **5e**

	4a′	**4b**	**4e′**	**5b**	**5e**
empirical formula	$C_{49}H_{37}N_5O_2Cl_2$	$C_{44}H_{27}N_4Br$	$C_{72}H_{54}N_6$	$C_{45}H_{27}N_4Br_3Cl_2$	$C_{44.5}H_{26.5}N_4Br_2Cl_{1.5}$
fw	798.77	691.63	1003.26	934.35	830.21
color	green	violet	green	violet	violet
habit	prismatic	prismatic	prismatic	prismatic	prismatic
cryst sys	triclinic	monoclinic	monoclinic	triclinic	monoclinic
space group	$P\bar{1}$	Cc	$P2_1/c$	$P\bar{1}$	$P2_1/c$
a, Å	14.637(2)	21.119(3)	15.5540(4)	12.880(3)	12.10(2)
b, Å	15.496(4)	12.021(4)	16.5407(5)	13.312(3)	26.36(6)
c, Å	10.462(7)	12.901(3)	20.4132(6)	12.87(1)	22.68(2)
α, deg	100.61(2)	90.00	90.00	109.66(4)	90.00
β, deg	108.21(3)	94.12(2)	96.7255(7)	111.15(5)	98.50(10)
γ, deg	64.58(2)	90.00	90.00	93.04(2)	90.00
V, Å^3	2032(2)	3266(1)	5215.6(2)	1899(2)	7153(18)
Z	2	4	4	2	8
radiation (λ, Å)			Mo Kα (0.710 73)		
T, °C	23.0	23.0	−180.0	15.0	20.0
D_C, g/cm^3	1.305	1.406	1.278	1.634	1.542
μ, cm^{-1}	2.069	13.019	0.751	33.762	2.425
R_1 (obs data)	0.106	0.045	0.067	0.108	0.076
R_{w2} (obs data)	0.149	0.036	0.106	0.128	0.028
GOF	2.171	1.810	1.379	0.840	3.020
independent reflecns	4817	4127	11938	5104	10753
obs reflecns	2963	2126	4889	3500	5937
params	543	440	793	463	917

1H, $J = 5.0$ Hz), 8.67 (d, 1H, $J = 5.0$ Hz), 8.69 (d, 1H, $J = 4.5$ Hz), 8.97 (m, 2H). ^{13}C NMR: δ 21.46, 21.49, 21.52, 21.54, 55.83, 116.77, 122.43, 122.90, 123.57, 124.45, 127.40, 127.43, 127.60, 127.73, 127.79, 128.09, 128.39, 128.43, 128.51, 128.96, 134.31, 134.61, 134.73, 134.92, 135.07, 135.42, 136.19, 137.24, 137.79, 137.81, 138.15,138.28, 138.56, 138.60, 138.74, 139.47, 139.95, 142.06, 144.43, 150.19, 156.61, 157.55, 157.79. UV/vis (CH_2Cl_2, λ_{max}): 661.5, 483.0, 371.5. FAB-MS: $m/z =$ 745.6 (calcd for $C_{49}H_{39}N_5O_3$ [M$^+$] 745.3053).

X-ray Crystallography. Crystallographic details are summarized in Table 7. Compound **4a′**: Crystals were obtained from $CHCl_3$−EtOH, and the data crystal was a dark green prism of approximate dimensions 0.4 × 0.1 × 0.1 mm ($C_{48}H_{35}N_5O_2{\cdot}CH_2Cl_2$). Data were collected at 15.0 °C on a Rigaku *R*-axis diffractometer using graphite monochromated Mo Kα radiation in the scan range $7.5° \le \theta \le 27.5°$. Of the 4817 reflections measured, 4817 were unique and 2963 had $F_o > 3\sigma F_o$.

Compound **4b**: Crystals were obtained from CH_2Cl_2−MeOH, and the data crystal was a dark violet prism of approximate dimensions 0.3 × 0.2 × 0.4 mm ($C_{44}H_{27}N_4Br$). Data were collected at 23.0 °C on a Rigaku Afc.7r diffractometer using graphite monochromated Mo Kα radiation in the scan range $7.5° \le \theta \le 27.6°$. Of the 4127 reflections measured, 3942 were unique and 2126 had $F_o > 3\sigma F_o$.

Compound **4e′**: Crystals were obtained from $CHCl_3$−EtOH, and the data crystal was a dark green prism of approximate dimensions 0.45 × 0.20 × 0.15 mm ($1.5C_{48}H_{36}N_4$). Data were collected at −180.0 °C on a Rigaku *R*-axis diffractometer using graphite monochromated Mo Kα radiation in the scan range $7.5° \le \theta \le 27.5°$. Of the 46 198 reflections measured, 11 398 were unique and 4889 had $F_o > 3\sigma F_o$.

Compound **5b**: Crystals were obtained from CH_2Cl_2−MeOH, and the data crystal was a dark violet prism of approximate dimensions 0.3 × 0.1 × 0.1 mm ($C_{44}H_{25}N_4Br_3{\cdot}CH_2Cl_2$). Data were collected at 15.0 °C on a Rigaku *R*-axis diffractometer using graphite monochromated Mo Kα radiation in the scan range $7.5° \le \theta \le 27.5°$. Of the 5104 reflections measured, 5104 were unique and 3500 had $F_o > 3\sigma F_o$.

Compound **5e**: Crystals were obtained from $CHCl_3$−EtOH, and the data crystal was a dark violet prism of approximate dimensions 0.3 × 0.15 × 0.1 mm ($C_{44}H_{26}N_4Br_2{\cdot}0.5CHCl_3$). Data were collected on a Rigaku *R*-axis diffractometer in the scan range $7.5° \le \theta \le 27.7°$. Of the 10 753 reflections measured, 10 753 were unique and 5937 had $F_o > 3\sigma F_o$. The structures were solved by direct methods and refined by full-matrix least-squares procedures with anisotropic thermal parameters for the non-hydrogen atoms. The hydrogen atoms were calculated in ideal positions. Solution and structure refinement calculations for the structures were performed using the teXsan crystallographic package of Molecular Structure Corp.

Acknowledgment. This work was supported in part by a Grant-in-Aid for Scientific Research (Grant No. 09640642 to H.F.) from the Ministry of Education, Science and Culture, Japan. We thank Dr. Motoo Shiro (RIGAKU) for the help of X-ray analyses.

Supporting Information Available: Figures showing UV/vis spectra for **4a′**, **4b**, **4c**, **5b**, and **5e**; ^{1}H NMR spectra of **4b**-d_{20} and **5b**-d_{20}; PM3 calculated HOMO−LUMO spin density of **4e′**; ^{13}C NMR spectra of NFPs (**4a′**, **4b**, **4c**, **4e**, **4e′**, **5b**, **5e**, and **6e′**); and UV/vis spectra of NCPs (**2c**, **3a′**, **3c**, **6a**, **6b**, **6c**, **6d** and **6e′**) tables listing X-ray crystallographic files, atomic coordinates and parameters, bond distances and angles, and least squares planes; and text describing crystallographic details for **2a′**, **4a**, **4b**, **4e′**, **5b**, and **5e** (PDF). This material is available free of charge via the Internet at http://pubs.acs.org.

JA000148I